Available online at www.sciencedirect.com

ScienceDirect

Energy Procedia 92 (2016) 576 – 584

Energy Procedia

6th International Conference on Silicon Photovoltaics, SiliconPV 2016

An electric model of cracked solar cells accounting for distributed damage caused by crack interaction

Marco Paggi[a*], Irene Berardone[a], Marco Martire[b]

[a]IMT School for Advanced Studies Lucca, Piazza San Francesco 19, 55100 Lucca, Italy
[b]Applied Materials, Via Postumia Ovest 244, 31048 Olmi di S. Biagio di Callalta, Italy

Abstract

Electric models based on a distributed series resistance along the grid line can be used to predict the current through the thickness of the Silicon solar cell, as well as the current and the voltage along the grid line. In the presence of a crack intersecting a finger, a localized electrical resistance dependent on the crack opening has to be introduced in that intersection point. In the present study, a refinement of these electric models is proposed by introducing a sheet resistance dependent on the amount of damage induced by cracks in the surrounding material. The proposed model is successfully validated in reference to experimental data on mono-crystalline Silicon solar cells with cracks artificially created by Vickers indentation, providing an insight into the electric degradation mechanisms caused by crack interaction phenomena.

Peer review by the scientific conference committee of SiliconPV 2016 under responsibility of PSE AG.

Keywords: One dimenstional electric model; Distributed damag; Vickers indentation; Cracks; Mono-crystalline Silicon

1. Introduction

In the last few years, the durability of photovoltaic (PV) modules emerged as an important issue to be debated by the scientific community [1-3]. International organizations and agencies are interested in the interpretation of laboratory and field degradation data of PV modules coming from different producers and installed in different climate zones [4]. For this reason, the understanding of the possible sources of losses in the energy production and the quantification of the degradation of a PV system are fundamental issues to establish appropriate business plans accounting for maintenance costs considering warranties when the underperformance of PV modules are above the producers' specifics. In addition to this, the durability issue is expected to become even more relevant in the next few years due to the rapid development of building integrated PV systems. In this work, we focus our attention on the damage caused by cracks in monocrystalline Silicon solar cells. The effects of cracks on solar cells are manifold,

Peer review by the scientific conference committee of SiliconPV 2016 under responsibility of PSE AG.
doi:10.1016/j.egypro.2016.07.022

including a linear decreasing of the short circuit current by increasing the inactive cell area [1,5,6] and an increase in the series resistance of the cell [2,7]. Potentially, if a crack crossing a finger (grid line) is sufficiently wide, an interruption of the electric flow to the busbars, or from the busbar in case of the electroluminescence (EL) test, may occur. In the present contribution, the one-dimensional model for the current distribution along a grid line in [8] is further generalized by considering not only the effect of cracks crossing the grid line as in [9], but also a distributed damaged region around the cracks. This is achieved by introducing a distributed resistance depending on the amount damage induced by cracks in the surrounding material. Experimental results are proposed to identify the model parameters and assess the important role of crack interaction on the introduced novel electric parameters.

2. Effect of cracks on the material proprieties of monocrystalline Silicon

Vickers micro-indentation is a suitable methodology to propagate cracks in Silicon solar cells that are similar to those induced by impacts [10, 11]. The typical shape of a Vickers indenter is a square-base diamond pyramid. The angle between opposite faces of the pyramid is 136°. This test is also called *diamond-pyramid hardness* (DPH) test, due to the shape of the indenter. The Vickers hardness provides a continuous scale of hardness, for a given load, from very soft metals with a DPH of 5 to extremely hard materials with a DPH of 1500 and, due to the geometric similarity of impressions made by the pyramid indenter, no matter their size, the DPH is independent of load [12].

After the insertion of cracks with this technique, nano-indentation tests have been performed in [11] to measure the material hardness in the surrounding region, showing a dependency of this material property on the distance from the main channel micro-crack, see the dots in Fig. 1, where H_{Si} denotes the hardness of the undamaged Silicon. This is the result of the pile up of dislocations in the surrounding material, of higher amplitude in the material region near the channel crack located at x=0. This experimental trend can be well fitted by an exponential decay of the type:

$$\frac{H}{H_{\mathrm{Si}}} = \frac{1}{\exp(x)^{a/H_{\min}} + 1} \tag{1}$$

where H_{Si}=10.5 GPa, H_{min}=7.1 GPa, and a=0.4, see the solid line in Fig. 1.

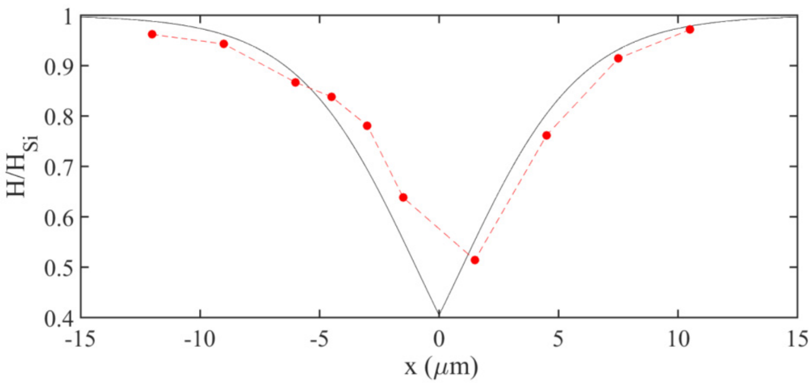

Fig. 1. Profile of the hardness near the channel crack located at x=0 (experimental data from [11], fitted by an exponential decay in Eq. (1) by the present authors, shown with solid line).

3. A one-dimensional electric model for monocrystalline Silicon cells with distributed damage

Under the assumption of an ideal semiconductor, which has homogeneous properties everywhere in the plane of the solar cell, the two-diode electric model proposed in [8] has been generalized in [9, 13] by considering a localized crack resistance dependent on crack opening. In this section, that electric model is further generalized in case of distributed damage in the Silicon solar cell surrounding the main channel cracks. The improved electric model allows the prediction of the current I_f (ξ) along the finger, for each position described by the coordinate ξ ranging from one busbar to the other (see Fig. 2). According to [8], in fact, the voltage is not constant, but it is a function of ξ due to a distributed resistance of the grid line, due to metallization and emitter resistances. Finally, for each voltage $V(\xi)$, the current $I_{tt,}$ through the thickness of the solar cell can be predicted by the single diode equation describing the physics of the semiconductor [9, 13]. In this section, this electric model is generalized by accounting for one or two intersecting cracks. From preliminary results in [9] it is found that a localized resistance at the position along the finger crossed by a crack has to be introduced, together with the spatial variation of the grid line resistance [8], to model experimental trends. By introducing for each finger a local reference frame with axis ξ directed along the finger direction and ranging from the first busbar at $\xi = 0$ to the second at $\xi = l$ (see Fig. 2), the surface density of electric current through the thickness of the solar cell originated in the semiconductor by the photovoltaic effect, I_{tt} (A/cm^2), the voltage V (V), and the linear density of current (per unit depth) along the finger, I_f (A/cm), depend on the position ξ due to a distributed series resistance ρ_S (Ω/cm^2) evaluated as the grid resistance R_{grid} (Ω/cm) divided by the spacing between two subsequent fingers.

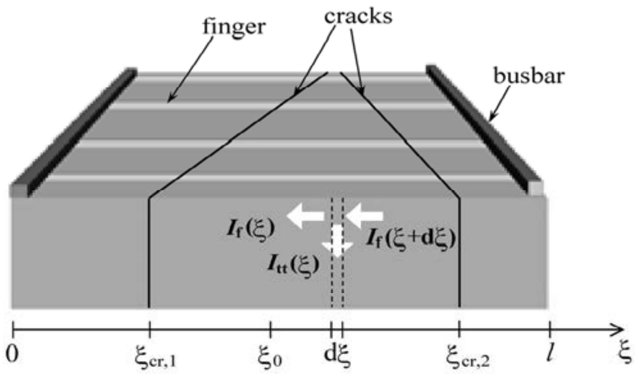

Fig. 2. A sketch of the solar cell with two cracks.

During the electroluminescence test, performed inside a dark room without sunlight and under a direct bias condition, the following ordinary differential equation relates the linear density of current along the finger to the variation in the voltage:

$$\frac{dV(\xi)}{d\xi} = V'(\xi) = -\rho_S I_f(\xi) \tag{2}$$

For continuity conditions on an infinitesimal portion of the grid line and the solar cell behind it, the derivative of the linear density of current along the finger has to be equal to the surface density of current passing through the solar cell thickness, i.e.:

$$\frac{dI_f}{d\xi} = -I_{tt}(\xi) \tag{3}$$

By manipulation of Eqs. (2) and (3), the following second order ordinary differential equation is derived:

$$\frac{d^2V(\xi)}{d\xi^2} = V''(\xi) = \rho_S I_{tt}(\xi) \tag{4}$$

The surface density of current through the thickness of the solar cell, I_{tt}, is herein approximated by a single diode model:

$$I_{\mathrm{tt}}(\xi) = I_{01}\exp\left(\frac{V(\xi) - R(\xi)I_{\mathrm{tt}}(\xi)}{n_1 V_{\mathrm{T}}}\right) \tag{5}$$

where I_{01} is the saturation current density, $n_1 \sim 1$ is the diode ideality factor, $V_{\mathrm{T}} = k_{\mathrm{B}}T/e$ is the thermal voltage dependent on the absolute temperature T, on the Boltzmann constant k_{B} and on the elementary electron charge e. The local sheet resistance in series with the diode is herein replaced by $R(\xi)$. This is usually treated as a simple constant in the existing formulations, and the voltage V is just varying along the finger due to the distributed grid line resistance. Here, we propose to use a non-constant value of $R(\xi)$ depending on the distance from the channel crack. The dependency of $R(\xi)$ for each crack can be assumed to be of exponential type, in line with the degradation of the material properties previously shown for hardness. This assumption leads, for two channel cracks located in $\xi = \xi_{\mathrm{cr1}}$ and $\xi = \xi_{\mathrm{cr2}}$, to the following expression, where the superposition of the damage effects of each individual crack is taken into account:

$$R(\xi) = \begin{cases} \exp\left[\left(\frac{\xi_{\mathrm{cr1}} - \xi}{l}\right)\right]^k R_{\mathrm{d1}} + \exp\left[\left(\frac{\xi_{\mathrm{cr2}} - \xi}{l}\right)\right]^k R_{\mathrm{d2}} + R'_{\mathrm{hom}}, & \text{for} \quad \xi < \xi_{\mathrm{cr1}} \\ \exp\left[-\left(\frac{\xi_{\mathrm{cr1}} - \xi}{l}\right)\right]^k R_{\mathrm{d1}} + \exp\left[\left(\frac{\xi_{\mathrm{cr2}} - \xi}{l}\right)\right]^k R_{\mathrm{d2}} + R'_{\mathrm{hom}}, & \text{for} \quad \xi_{\mathrm{cr1}} \le \xi \le \xi_{\mathrm{cr2}} \\ \exp\left[-\left(\frac{\xi_{\mathrm{cr1}} - \xi}{l}\right)\right]^k R_{\mathrm{d1}} + \exp\left[-\left(\frac{\xi_{\mathrm{cr2}} - \xi}{l}\right)\right]^k R_{\mathrm{d2}} + R'_{\mathrm{hom}}, & \text{for} \quad \xi > \xi_{\mathrm{cr2}} \end{cases} \tag{6}$$

In Eq. (2), R_{d1}, R_{d2}, R'_{hom}, and k are the free parameters of the model. Furthermore, a localized resistance R_{cr} is considered at the point where a crack crosses the finger, as in [9].

In the case of an intact cell, it is sufficient to set R_{d1}, R_{d2} equal to zero and $R(\xi) = R'_{\mathrm{hom}}$ to recover the one-dimensional electric model in [9,13] as special case.

Since Eq. (5) has an implicit form, the current I_{tt} cannot be obtained in a closed form, and the Newton-Raphson incremental-iterative scheme is invoked. Considering I_{tt}^0 = 0.2 mA/cm^2 as the starting value, convergence is achieved when the error in the norm of the computed I_{tt} is less than a prescribed tolerance. Due to the consistent update of the tangent, the rate of convergence is quadratic and few iterations are needed to achieve an error within the machine precision.

Numerical integration of the ODE in Eq. (4) is performed by discretizing the grid line in nodes with a regular spacing $\mathrm{d}\xi$. The starting point for the integration is the point at $\xi = \xi_0$ where the voltage is minimum, say V_0. For a finger not intersected by any crack, this point is located in the middle between two busbars ($\xi_0 = l/2$). For a finger intersected by a crack, ξ_0 is a free parameter to be identified by matching the value of the voltage at the busbars, which is a known imposed value in the EL test (see Fig. 2). For a tentative value of ξ_0, whose initial guess can be $\xi_0 = l/2$, and the corresponding voltage, $V(\xi_0) = V_0$ which is in general lower than the applied voltage at the busbars (0.7 V for a typical EL test), the integration path is divided into two parts. In reference to Fig.2, the first part is comprised between ξ_0 and the busbar on the left (ξ=0), while the second part ranges from ξ_0 and the busbar on the right (ξ=1). The current density $I_{\mathrm{tt}}(\xi)$ is assumed to be constant within each integration interval $\mathrm{d}\xi$. Under such a hypothesis, the voltage profile within each interval $\mathrm{d}\xi$ is parabolic and the following equations hold:

$$\begin{aligned} V(\xi + \mathrm{d}\xi) &= V(\xi) + V'(\xi)\mathrm{d}\xi + \frac{V''(\xi)}{2}\mathrm{d}\xi^2 \\ V'(\xi + \mathrm{d}\xi) &= V'(\xi) + V''(\xi)\mathrm{d}\xi \\ I_{\mathrm{f}}(\xi + \mathrm{d}\xi) &= I_{\mathrm{f}}(\xi) + I_{\mathrm{tt}}(\xi)\mathrm{d}\xi \end{aligned} \tag{7}$$

where (') and ('') indicate the first and second order derivatives with respect to ξ. Referring to the integration in the first region (from $\xi = \xi_0$ to $\xi = 0$), the boundary conditions are given by:

$$V(\xi_0) = V_0 \quad \text{and} \quad V'(\xi_0) = 0 \tag{8}$$

The vertical current $I_{tt}(\xi)$ is then computed with the Newton-Raphson algorithm applied to Eq.(5). In the next step, the voltage $V(\xi–\mathrm{d}\xi)$, its derivative $V'(\xi–\mathrm{d}\xi)$, and the linear density of current along the finger, $I_f(\xi–\mathrm{d}\xi)$ are evaluated at the new integration point $\xi-\mathrm{d}\xi$ according to Eq. (6). The negative sign of $\mathrm{d}\xi$ is due to the fact that integration is performed from $\xi = \xi_0 > 0$ to $\xi = 0$.

When, in the integration path, the crack crosses the finger at the point $\xi_{cr,1}$, an additional localized resistance $R_{cr,1}$ is introduced, dependent on its crack opening [13], in agreement with experimental findings in [10] and recently confirmed by optical microscope images and electric measurements in [14]. Indeed, the effect of a crack on I_{tt} was evident in the EL images reported in [10], being possible to correlate the brightness of the EL image to I_{tt} [15]. Indeed, for a sufficient large crack opening displacement, a discontinuity in the grey-scale of the EL image takes place [13]. Due to the presence of the concentrated resistance related to the crack, a discontinuity in the voltage distribution occurs in correspondence of this crack position, $\xi_{cr,1}$:

$$V(\xi_{cr}^+) = V(\xi_{cr}^-) + R_{cr} I_f(\xi_{cr}) \tag{9}$$

After this voltage discontinuity, the integration proceeds as previously done before the intersection with the crack. Regarding the integration in the second region, from $\xi = \xi_0$ up to $\xi = l$, the same procedure as before is applied to compute $V(\xi+\mathrm{d}\xi)$, $V'(\xi+\mathrm{d}\xi)$ and $I_f(\xi+\mathrm{d}\xi)$ in the point with coordinate $\xi+\mathrm{d}\xi$, starting from the boundary condition imposed at $\xi = \xi_0$. Again, in case of another crack crossing the finger at $\xi = \xi_{cr,2}$, the voltage has a discontinuity in that point due to the concentrated resistance $R_{cr,2}$.

4. Experimental evidence and validation

Cracks are induced in mono-crystalline Silicon solar cells by Vickers indentation (see Fig. 3a). The EL images taken before and after the indentation test are shown in Fig. 3b and 3c, respectively.

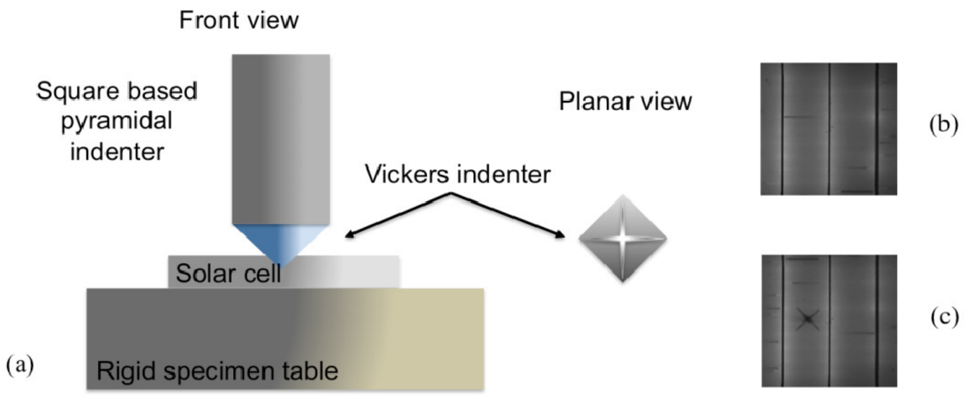

Fig. 3. (a) Sketch of the Vickers micro-indenter. (b) EL image of the solar cell before indentation; (c) EL image after indentation.

The proposed electric model is applied to four fingers crossed by the radial cracks, at different distances from the central point of Vickers indentation. The distribution of the current flowing through the thickness of the solar cell predicted by the present model, I_{tt}, is shown in Fig. 4 for these fingers. The following parameters are set for all of the cases: $R'_{hom} = 0.1\ \Omega\mathrm{cm}^2$, $V_T = 25$ mV, $\rho_s = 0.138\ \Omega$, $I_{01} = 1.48\mathrm{x}10^{-12}$ A/cm^2, $V_0 = 0.589$ V.

The predicted current is compared with the experimental value deduced from the EL image according to the method discussed in [9], see Fig. 4. A fair good agreement between model predictions and numerical results is achieved. The values of the resistances for the two cracks identified by matching the experimental data are plotted in Fig. 5 vs. the distance *d* between the two cracks.

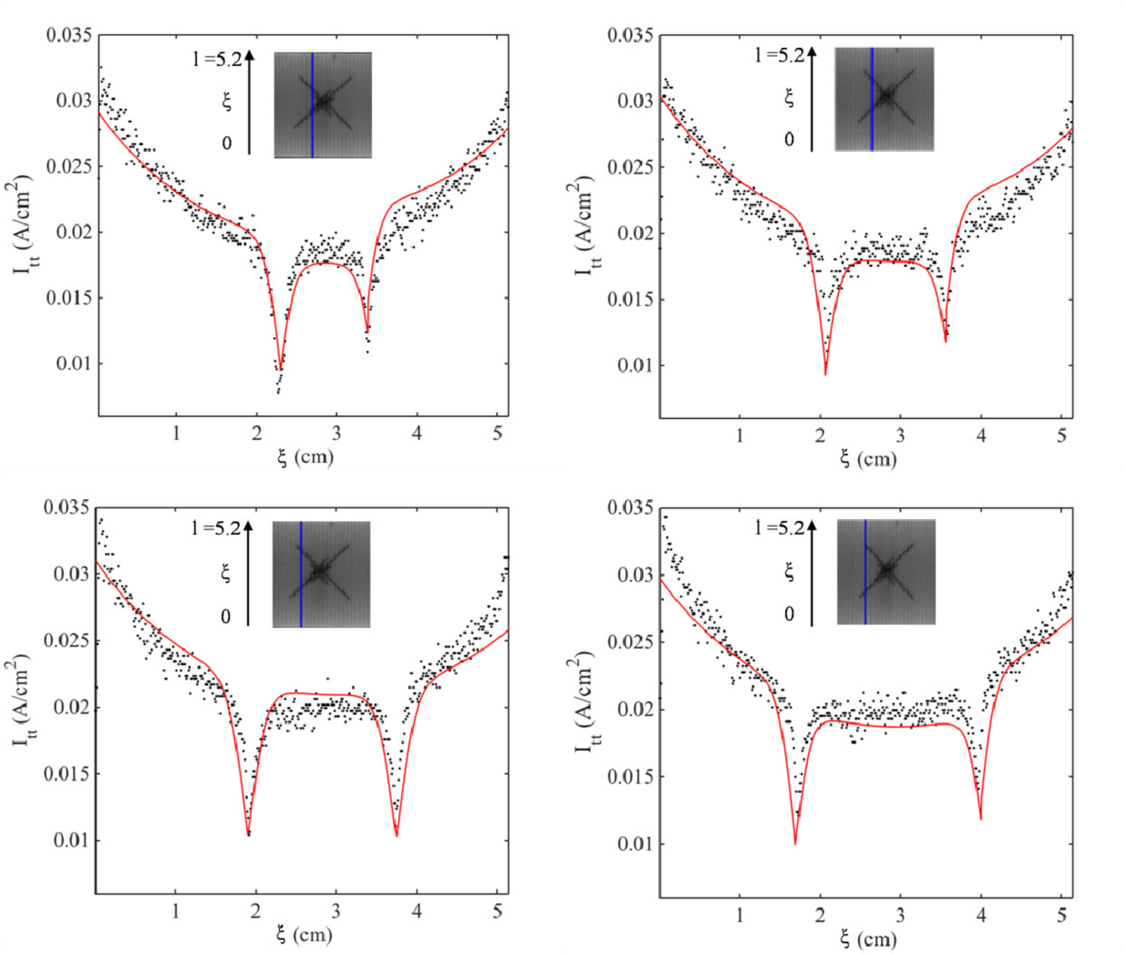

Fig. 4. Current through the thickness of the solar cell vs. position along the finger. Experimental values are shown with dots, model predictions with continuous red line.

Results show that the localized resistances R_{cr1} and R_{cr2} are almost independent of *d* (see Fig. 5a), in agreement with the expectation that they should depend on crack opening only. On the other hand, the resistances R_{d1} and R_{d2} are decreasing functions of the distance between cracks (see Fig. 5b), which implies a higher degradation of the Silicon properties due to the effect of crack interaction enhancing dislocations pile up.

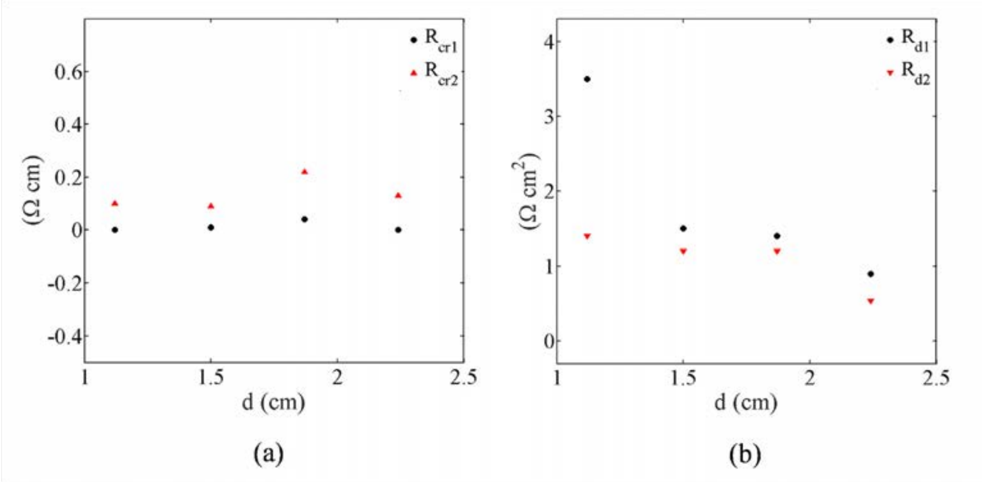

Fig. 5. Model resistances vs. distance between cracks: (a) localized crack resistances; (b) distributed crack resistances.

5. Comparison with the electric model with localized resistance only

In this section, a comparison between the generalized electric model for distributed damage (DD) and the electric model which considers the localized resistance at the crack position only (LR) is proposed. The two models are applied to mono-crystalline Silicon cells embedded in semi-flexible modules made of 2 rows of 5 cells each. Cracks were induced via impact tests to simulate hail impacts [10]. Loaded and unloaded configurations have been considered in order to change the stress field in the cells. The application of a bending load to the module determines an increase of the crack opening displacement of the pre-existing cracks [13]. The distribution of the current flowing through the thickness of the solar cell predicted by the two models, I_{tt}, is shown in Fig. 6 a finger crossed by a single crack at ξ~2.

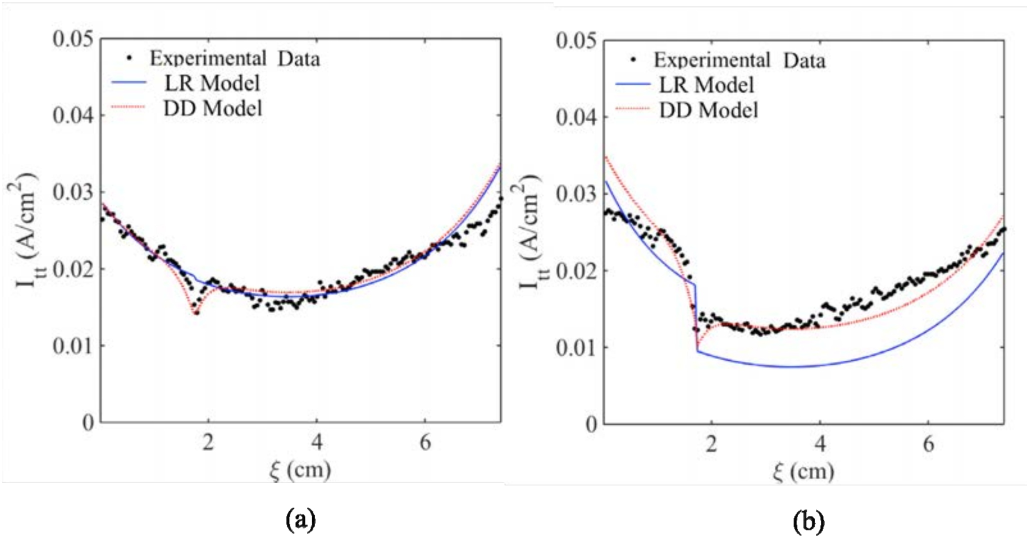

Fig. 6. Comparison between the predictions of the model with localized resistance only, of the model with also distributed crack resistance, and experimental data. (a) Undeformed PV module; (b) Deformed PV module due to bending.

The following parameters have been set for the two models: $V_T = 25$ mV, $\rho_s = 0.138\ \Omega$, $I_{01} = 1.48\text{x}10^{-12}$ A/cm^2. The values of the other parameters, specific for each model, are collected in Tab.1.

Table 1 Model parameters for the example in Fig. 6.

Model	Condition	x_{min} (cm)	x_{cr1} (cm)	V_0 (V)	R_{cr1} (Ωcm)	R_{cr2} (Ωcm^2)	R_{ohm}' (Ωcm^2)	k (-)
LR	Undeformed	3.47	1.65	0.581	0.02	-	0.1	-
DD	Undeformed	3.47	1.65	0.581	0.02	0.65	0.1	40
LR	Deformed	3.47	1.7	0.597	0.35	-	0.1	-.
DD	Deformed	3.47	1.7	0.597	0.35	0.65	0.1	40

The density of current flowing through the thickness obtained with the LR model (blue solid line) and with the DD model (red dashed line) is compared with the experimental data along the same grid line (black dots in Figs. 6a and 6b, for the unloaded and loaded configurations, respectively). As expected, the results in Fig. 6 show that the model accounting for distributed damage is more accurate in capturing the experimental trend.

6. Conclusions

A novel electric model with spatially varying distributed resistance (DR) accounting for damage in the material surrounding a channel crack has been proposed to predict the current through the thickness of cracked Silicon solar cells, as well as the current and the voltage along the grid line. To validate the DR model, Vickers tests on monocrystalline Silicon solar cells have been performed to generate a configuration where two cracks are crossing aa finger. The present formulation has been proved to be very accurate in modelling the electric response. Moreover, in case of a single crack induced by impact loads, the present model is found to be more accurate that the original model with localized resistance only (LR), both in the simulation of the electric response of the solar cell without bending deformation, and of the same solar cell loaded in bending to increase the amount of crack opening.

Acknowledgements

The present research has received funding from the European Research Council under the European Union's Seventh Framework Programme (FP/2007-2013) / ERC Grant Agreement n. 306622 (ERC Starting Grant "Multi-field and multi-scale Computational Approach to Design and Durability of PhotoVoltaic Modules"-CA2PVM).

References

[1] Koentges M, Kunze I, Kajari-Schroeder S, Breitenmoser X, Bjørneklett B. The risk of power loss in crystalline silicon based photovoltaic modules due to micro-cracks. Sol Energ Mat Sol Cells 2011;95:1131-37.
[2] Kajari-Schroeder S, Kunze I, Eitner U, Koentges M. Spatial and orientational distribution of cracks in crystalline photovoltaic modules generated by mechanical load tests. Sol Energ Mat Sol Cells 2011;95:3054-59.
[3] Kajari-Schroeder S, Kunze I, Koentges. Criticality of cracks in PV modules. Energy Procedia 2012;27:658-63.
[4] IEA PVPS Task 13, Performance and reliability of photovoltaic systems. Subtask 3.2: review of failures of photovoltaic modules. ISBN 978-3-906042-16-9.
[5] Kim K-H, Kasouit S, Johnson EV, Cabarrocas PR. Substrate versus superstrate configuration for stable thin film silicon solar cells. Sol Energ Mat Sol Cells 2013;119:124-8.
[6] Kim K-H, Johnson EV, Cabarrocas PR. Irreversible light-induced degradation and stabilization of hydrogenated polymorphous silicon solar cells. Sol. Energ. Mat. Sol. Cells 2012;105:208-12.
[7] Khatri R, Agarwal S, Saha I, Singh SK, Kumar B. Study on long term reliability of photo-voltaic modules and analysis of power degradation using accelerated aging tests and electroluminescence technique. Energy Procedia 2011;8:396-01.
[8] Breitenstein O, Rißland S. A two diode model regarding the distributed series resistance. Sol. Energ. Mat. Sol. Cells 2013;110:77-86
[9] Berardone I, Corrado M, Paggi M. A generalized electric model for mono and polycrystalline silicon in the presence of cracks and random defects. Energy Procedia 2014;55:22-9.
[10] Paggi M, Berardone I, Infuso A, Corrado M. Fatigue degradation and electric recovery in Silicon solar cells embedded in photovoltaic modules. Scientific Reports 2014;4. 4506; DOI:10.1038/srep04506.

[11] Kulshreshtha KP, Youssef KM, Rozgonyi G. Nano-indentation: A tool to investigate crack propagation related phase transitions in PV silicon. Sol Energ Mat Sol Cells 2012;96:166-72.
[12] Dieter GE. Mechanical metallurgy. 3rd ed. University of Michigan: McGraw-Hill;1986.
[13] Paggi M, Corrado M, Berardone I. A global/local approach for the prediction of the electric response of cracked solar cells in photovoltaic modules under the action of mechanical loads. Eng Frac Mec 2016; doi:10.1016/j.engfracmech.2016.01.018
[14] Kaesewieter J, Haase F, Larrodé MH, Koentges M. Cracks in solar cell metallization leading to module power loss under mechanical loads. Energy Procedia 2014;55:469-477.
[15] Fuyuki T, Kondo H, Kaji Y, Ogane A, Takahashi Y. Analytic findings in the electroluminescence characterization of crystalline silicon solar cells. J Appl Phys 2007;101:023711.